IR-Assisted Discharge Initiation in Pulsed Plasma Thrusters

James E. Cooley[*] and **Edgar Y. Choueiri**[†]
Electric Propulsion & Plasma Dynamics Lab (EPPDyL)
Mechanical and Aerospace Engineering Department
Princeton University, Princeton, NJ 08544

AIAA-2002-4274[‡]

Abstract

It is demonstrated that a discharge can be initiated in a pulsed plasma thruster (PPT) at an undervoltage by shining an IR laser pulse on the thruster's backplate. The technique has the potential for achieving uniform and erosion-free discharge initiation. Three candidate mechanisms are investigated: thermionic emission, cathode vaporization, and gas desorption. Mass spectroscopic measurements and theoretical calculations implicate water desorption from the backplate as the likely explanation for the observed effects. It is then shown that while thermionic emission was not operative in the experiments, it can be used as the basis of the design of a discharge initiator.

1 Introduction

The idea of using a laser to initiate pulsed plasma thruster (PPT) discharges was introduced by Berkery and Choueiri.[1] The motivation is to explore a possible replacement for spark plugs as a method of discharge initiation. Spark plugs have high erosion rates which limit their lifetime[2] and produce azimuthally non-uniform current sheets which hinder thruster efficiency.[3]

The original idea involved using an ultraviolet laser pulse to create a pulse of electrons from the backplate of a PPT through the photoelectric effect. That electron pulse would alter the space charge characteristics of the discharge gap, thus lowering the breakdown voltage. If the discharge gap was initially placed at an undervoltage, a voltage slightly less than that required for breakdown without the electron pulse, and that undervoltage was greater than the breakdown voltage necessary with the electron pulse, then the electron pulse would have successfully initiated the discharge.

Berkery and Choueiri attempted to achieve a breakdown by shining ultraviolet laser pulses on a magnesium backplate fixed to the cathode of an undervoltaged GFPPT in an argon atmosphere, but they failed to initiate a discharge in this manner due to difficulties in properly conditioning the surface . They were, however, able to achieve a breakdown with a laser operating at an infrared wavelength. Since infrared photons do not possess enough energy to photoelectrically remove electrons from a magnesium surface, the mechanism behind this discharge was unclear.

[*]Graduate Research Assistant. Member AIAA.
[†]Chief Scientist at EPPDyL, Associate Professor, Applied Physics Group. Associate Fellow AIAA.

The goal of the research described in this paper was to identify the mechanism by which infrared laser pulses were able to induce breakdowns and explore its dependencies with the ultimate practical goal of determining whether or not this mechanism would be a viable method of thruster discharge initiation.

We considered several possible candidates for the breakdown mechanism. It was thought that an infrared laser pulse may heat the surface to the point that significant thermionic emission of electrons might occur. This electron pulse then might be enough to achieve a breakdown in the same manner as the photoelectric pulse initially considered. We also considered the possibility that each laser pulse might vaporize a small portion of the backplate material. The resulting magnesium vapor would be easier to ionize than the background argon and thus the breakdown would be achieved at the undervoltage. Similarly, we hypothesized that the heat from the laser pulse might release water vapor or other gases that had been absorbed into the bulk of the backplate.

We begin by describing the setup, methodology, and results of a series of experiments designed to illuminate the discharge mechanism. We then present a theoretical investigation of the interaction of the laser pulse with the backplate surface. It includes calculations of threshold energies below which thermionic emission and vaporization will not occur. In addition, we devise a functional relationship between the laser pulse energy and the flux of outgassed materials with the goal of explaining our experimental results. Finally, we present our conclusions on how the infrared-induced discharge works and how one might use this information to design a new initiation system for PPTs.

2 Experimental Setup

Experiments were carried out in a bell jar vacuum facility outfitted with a mechanical pump, diffusion pump, and refrigerated baffles. The facility is capable of reaching pressures as low as 2×10^{-4} Torr.

We used a Continuum Nd:YAG laser with fundamental of 1064nm in the infrared. The spot size of the laser is 1 cm and pulses with energies varying from 10 mJ to 500 mJ were used. The laser's flashlamps were pulsed at 10 Hz and the Q-switched laser pulse width was 8ns.

The pulsed plasma thruster used in these experiments is called PT4 and was developed in collaboration with Science Research Labs.[4] It has a coaxial geometry with the center electrode acting as the cathode and the outer electrode as the anode (Figure 1). The magnesium backplate is fixed to the cathode and held at cathode potential. We did not use the thruster's gas feed system or capacitor bank in any experiments; the thruster was strictly employed as a discharge gap with the appropriate geometry. This thruster was outfitted with a ceramic disc heater. Originally intended as part of a photocathode cleaning procedure, this heater was used as part of the control of the experiment described in Section 3.1.

Diagnostics included a UTI 100C Precision Mass Analyzer and a Scientech 362 laser power meter.

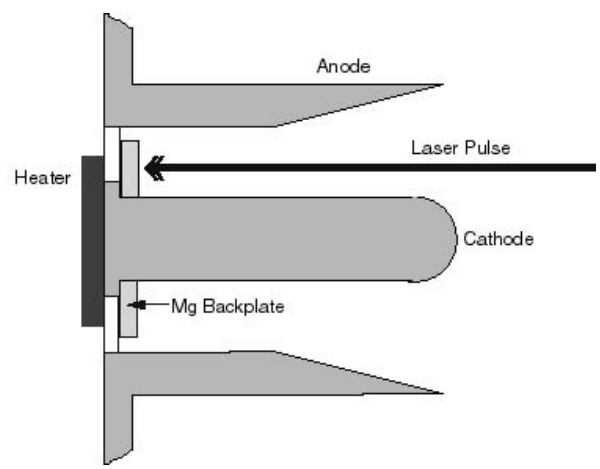

Figure 1: Schematic of the thruster used in experiments.

3 Experimental Methods and Results

Laser-induced discharges were produced in the following manner: the thruster was placed in the vacuum vessel which we then pumped down to 2×10^{-4} Torr, flushed three times with argon, and filled to the desired pressure. The voltage on the thruster was

then gradually increased until a breakdown occurred. This was repeated several times and the results averaged to calculate the breakdown voltage. The voltage was then decreased to the desired undervoltage, determined in terms of a percentage of the breakdown voltage. Single laser pulses were then directed onto the backplate and pulse energy was increased until a breakdown repeatably occurred. The laser was then set into a repeating pulsed mode and the average power was measured with the laser power meter.

Initial experiments achieved breakdowns with pulse energies as low as 10 mJ for a 3% undervoltage at a pressure of 500 mTorr. Since the model we present in Sections 4.2.2 and 4.2.3 predicts no thermionic current or surface vaporization at these power levels, we proceeded with the hypothesis that the effect was attributed to surface desorption.

3.1 Effect of Outgassing on Laser Pulse Energy Requirement

In order to measure the effect of outgassing on the laser pulse energy required for breakdown, we performed the following experiment. The thruster was placed in the vacuum vessel which was then pumped to its minimum pressure of 2×10^{-4}Torr. The heater was then turned on to raise the backplate temperature to 150^oC. The minimum laser pulse energy at which a breakdown could be repeatably achieved was then measured, and this was repeated at various times throughout the experiment. The results of that experiment are presented in Figure 2.

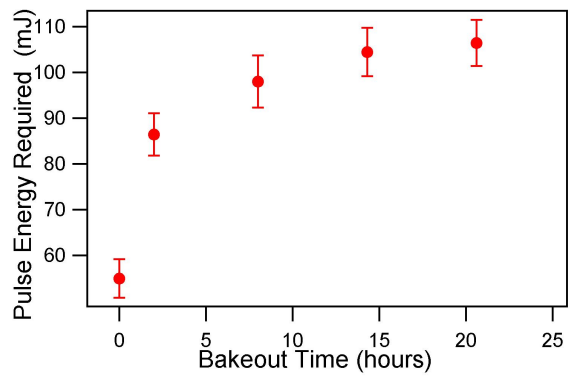

Figure 2: Measured minimum laser pulse energy required for breakdown as a function of bakeout time.

3.2 Mass Spectrometry

In order to determine the composition of desorbed gases, we performed mass spectrometry using a residual gas analyzer (RGA). The thruster was placed in the vacuum vessel which was pumped down to its minimum pressure. Its heater was then turned on to raise the backplate temperature to approximately 150^oC and the RGA was used to measure the molecular mass spectrum ranging from 1 to 100 amu. The bakeout period lasted approximately 6 hours. Figure 3 shows the relative heights of mass peaks that have been attributed to various species as a function of bakeout time. Each peak height is normalized to the height of the peak associated with diatomic nitrogen to give a relative partial pressure. Included species are water, diatomic oxygen, argon, and several hydrocarbons that are commonly found dissociative products of diffusion pump oil, mechanical pump oil, or vacuum grease, all of which are employed in the vacuum facility. All species presented were chosen because they exhibited interesting behavior and no significantly relevant peaks were left out.

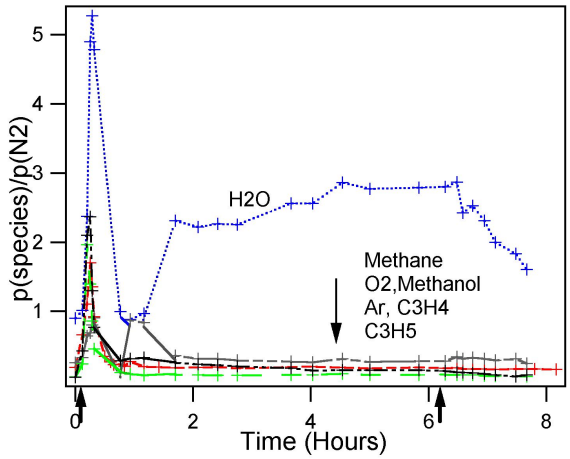

Figure 3: Relative partial pressures of various species as a function of bakeout time. The arrows indicate when when the heater was switched on and off.

Most of the species that outgassed did so completely within the first hour of baking. The notable exception is water, which dominated the outgassed mixture during the entire experiment. After approximately 90 minutes, water remained as the only species that outgassed significantly and continued to do so until the heater was turned off at approximately 6 hours.

4 Theory

4.1 Discharge Initiation Mechanisms

The current in gas-filled region between biased electrodes is given by [5]

$$i = \frac{i_0 e^{\alpha d}}{1 - \gamma(e^{\alpha d} - 1)}, \tag{1}$$

where α, called the Townsend ionization coefficient, is the number of ionizing collisions per unit length, d the width of the gap and γ the secondary electron emission coefficient from the cathode. The initial current, i_0, could be a photoelectric current from the walls or might be the result of cosmic rays or other ionizing phenomena. If we define a breakdown parameter,

$$\mu = \gamma[exp(\alpha d) - 1], \tag{2}$$

we see that as $\mu \rightarrow 1$, the discharge current becomes infinite. This is the Townsend breakdown criterion and marks the point at which the creation of electrons by ionization and secondary emission becomes self-sustaining. We hope to manipulate the breakdown by changing the initial current, which does not appear explicitly in the breakdown criterion. However, Berkery and Choueiri[1] describe a numerical model[1] that shows that a pulse of electrons introduced into an undervoltaged discharge gap will introduce a space charge in the gap and change the likelihood of ionization. Thus the initial current dependence is implicit in the Townsend ionization coefficient α. While this model was intended to treat pulses of electrons released photoelectrically, it does not specify any requirements on the source of the electron pulses. It is therefore clear that current emitted thermionically should be able to initiate a breakdown. We will also see, however, that all of the discharge mechanisms under consideration involve introducing electron pulses in some way. Thus, Berkery's and Choueiri's model remains appropriate.

The proposed mechanism by which released gases, be they magnesium vapor or desorbed gases, might initiate a breakdown relies on a requirement that the released gases are more likely ionized than the argon background. Free electrons in the undervoltaged gap are always accelerated by the applied filed, but they do not reach the energy required to sustain an amplifying avalanche. When a new gas with a higher α is introduced, however, ionization becomes more likely and the avalanche can propagate among that species. This "mini-avalanche" performs the same function as the electron current pulse considered in the model.

The Townsend ionization coefficient, α, is a function of pressure and electric field as given by [6]

$$\alpha = Ape^{-Bp/E}. \tag{3}$$

The constants A and B are determined by the gas and are presented in Table 1 for argon and water. Raising the ionization constants will lower the breakdown voltage. Constants A and B are not known for magnesium vapor, but the first ionization energy is presented along with those for argon and water. Based

on the ionization energy, it seems likely that magnesium vapor would ionize more frequently than argon. As a result, we expect that the introduction of water into an appropriately undervoltaged argon discharge gap should initiate a breakdown, and it seems reasonable to suggest that the introduction of magnesium would do the same.

	A [1/cmTorr]	B [V/cmTorr]	ε_I [eV]
A	12	180	15.8
H_2O	13	290	12.6[7]
Mg	-	-	7.65[8]

Table 1: Townsend ionization constants for argon and water and first ionization energies for argon, water and magnesium. All values are from von Engel[9] except where noted.

4.2 Effects of Laser Radiation on the Surface

The laser used for this experiment was a Q-switched Nd:Yag laser operating at 1064 nm with a pulse width of 8 ns. The spot size of the laser is 1 cm and pulses with energies varying from 10 mJ to 500 mJ were used.

Because of their short duration, Q-switched laser pulses have a high irradiance, or power per unit area, but do not heat the surface as effectively as a longer pulse with a lower irradiance.

4.2.1 Temperature Distribution

We begin by calculating the temperature in the metal as a function of depth during the laser pulse . We assume that the heat flow is one dimensional, which is will later be justified on the basis that the dimension of heat penetration is much smaller than the width of the beam. We also assume that the pulse energy is fully absorbed into the metal.

The differential equation for heat flow in a semi-infinite rod with a heat addition function $A(x,t)$ is[10]

$$\frac{\partial^2}{\partial x^2}T(x,t) - \frac{1}{\kappa}\frac{\partial}{\partial t}T(x,t) = -\frac{A(x,t)}{K}, \quad (4)$$

where T is the temperature, κ the thermal diffusivity, and K the thermal conductivity. If the surface is at $x = 0$, the initial and boundary conditions are

$$\begin{aligned} T(x,0) &= 0 \\ T(\infty,t) &= 0 \end{aligned} \quad (5)$$

We write our heating function as:

$$A(x,t) = F(t)(1/\delta)e^{-x/\delta}, \quad (6)$$

where F(t) is the absorbed laser irradiance in W/cm^2 and δ the skin depth of the metal.

Equation (4) is solved using Duhamel's principle, which involves finding the solution for which the temporal pulse shape is a flat step function at $t = 0$. For metals, which have high optical absorption, we get a solution:[10]

$$T(x,t) = \frac{\kappa^{1/2}}{K\pi^{1/2}}\int_0^t \frac{F(t-\tau)\exp(-x^2/4\kappa\tau)}{\tau^{1/2}}d\tau. \quad (7)$$

We assume that the laser pulse has the shape:

$$F(t) = I_{\text{peak}}(\frac{t}{T_{width}})^2 \exp(\frac{-2t}{T_{width}}). \quad (8)$$

Using this laser pulse shape, we numerically integrate Equation (7) to find the temperature distribution in the magnesium surface. Figure 4 is a plot of temperature versus depth with time as a parameter for an 8 ns pulse of energy 170 mJ.

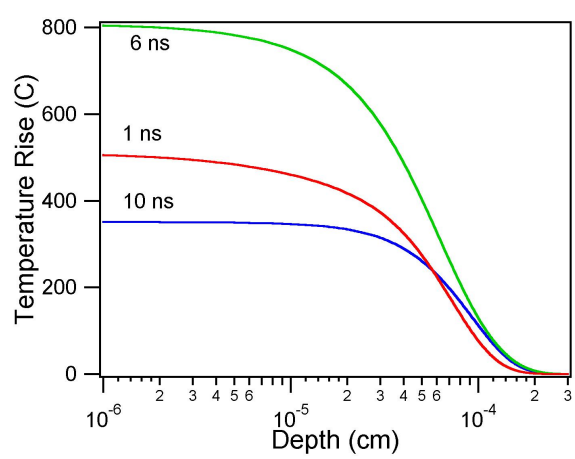

Figure 4: Temperature distribution in the metal at various times for a laser pulse with $T_{width} = 8ns$ and a pulse energy of 170 mJ.

Note that no significant heating occurs beyond 10^{-3} cm. Since the laser spot size is 1 cm, our assumption of one-dimensionality is valid.

4.2.2 Thermionic Electron Emission

Thermionic electron current density is a function of surface temperature as given by Richardson's equation :[11]

$$j = AT^2 \exp\left(-\phi/kT\right), \tag{9}$$

where j is the current density in A/cm^2, ϕ is the work function of the metal, and A is a constant equal to $60.2A/(cm^2C^2)$. Magnesium has an electron work function of 3.7 eV.

From this calculation and equation (9) we calculate the maximum thermionic electron current as a function of laser pulse energy; these results are presented in Figure 5.

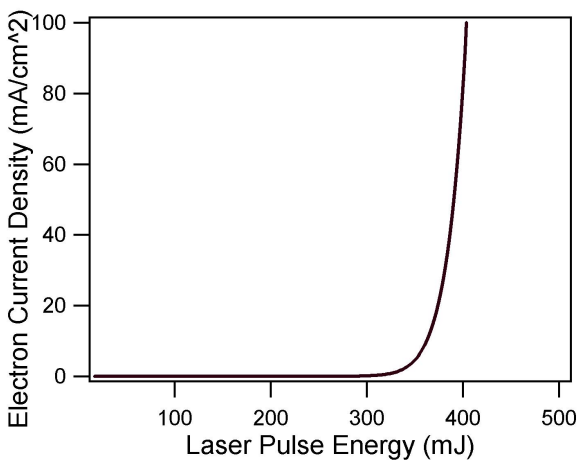

Figure 5: Maximum electron current density as a function of laser pulse energy.

From Figure 5 we see that there is essentially no thermionic electron emission until the pulse energy gets above 300 mJ.

4.2.3 Vaporization

Figure 6 is a plot of maximum surface temperature rise versus pulse energy. The boiling point of magnesium is 1100° C. We can see from this plot that the magnesium surface does not pass the boiling point for pulse energies below 250 mJ.

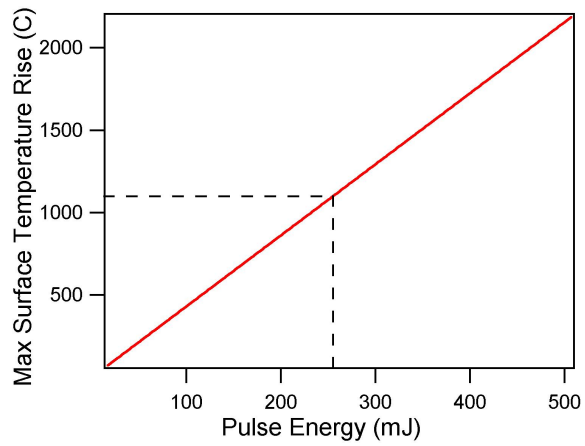

Figure 6: Maximum surface temperature as a function of pulse energy. The dotted line represents the boiling point of magnesium.

4.2.4 Desorption

As the laser heats the backplate surface, gas molecules trapped in adsorption sites on the surface will be released. We will begin by deriving a relationship between laser pulse energy and flux of desorbed gas with the surface concentration of that gas as a parameter. We will then use diffusion theory to understand how the surface concentration will change over a long outgassing period. This theoretical analysis is presented as an effort to assemble a model that describes the results of the outgassing experiment we describe in Section 3.1.

We assume that the desorption process is simple molecular desorption of the type described by the first order reaction:

$$M_{\text{adsorbed}} \rightleftharpoons M_{\text{gaseous}}. \tag{10}$$

Desorption of water from the magnesium surface is an example of this reaction. The rate of desorption is then described by [12]

$$R = -\frac{dN}{dt} = kN, \tag{11}$$

where N is the surface concentration of the adsorbed species and k is the reaction rate constant given by [12]

$$k = ne^{-\varepsilon_{\rm des}/RT}. \tag{12}$$

Here $\varepsilon_{\rm des}$ is the activation energy for desorption and n is the "attempt frequency" of overcoming the desorption barrier. This can be taken as the frequency of vibration between the molecule and the substrate; each stretching of the bond can be considered an attempt at overcoming the potential barrier. This frequency is usually on the order of $10^{13}s^{-1}$.[12] The activation energy for desorption for water in MgO is 55 kJ/mol .[13]

Combining Equations (11) and (12) gives the desorption flux as a function of temperature and surface concentration:

$$\Gamma_{des} = nNe^{-\varepsilon_{des}/RT}. \tag{13}$$

We now wish to find the surface concentration as a function of time during a long outgassing period. We assume that the metal initially contains a uniformly distributed concentration of gas C_0 which we leave as a free parameter. We also continue to treat the problem as a semi-infinite solid in one dimension. The process by which gas reaches the surface is diffusion, which is described by Fick's law [14]

$$\frac{\partial}{\partial x}\left(D\frac{\partial C}{\partial x}\right) = \frac{\partial C}{\partial t}. \tag{14}$$

C is the concentration in molecules/cm^3 and D is the diffusion constant. If x is the depth coordinate and we set the surface at $x = 0$, we can solve this equation to get the concentration as a function of depth and time.

$$C(x,t) = C_0 {\rm erf}[x/2(Dt)^{1/2}]. \tag{15}$$

We also note that the flux of molecules to the surface as a function of time is given by

$$\Gamma(t) = D\left(\frac{\partial C(x,t)}{\partial x}\right)_{x=0}, \tag{16}$$

where Γ is in molecules/s cm^{-2}. Using Equation (15), we get the diffusive flux to the surface as a function of time:

$$\Gamma(t) = C_0\left(\frac{D}{\pi t}\right)^{1/2}. \tag{17}$$

The surface concentration will be determined by a balance between diffusive flux to the surface and desorptive flux from the surface:

$$\left(\frac{dN}{dt}\right)_{\rm net} = \left(\frac{dN}{dt}\right)_{\rm diffusive} - \left(\frac{dN}{dt}\right)_{\rm desorptive}. \tag{18}$$

There are three relevant timescales in our problem. It is assumed that the time in which the laser removes the desorptive flux from the surface is much faster than the timescale on which a steady-state surface concentration is reached. That timescale is then assumed to be much faster than the time scale on which the diffusive flux changes. Thus, during the time it takes to reach a steady-state surface concentration, the magnitude of the diffusive flux doesn't change. We therefore treat the value of diffusive flux as constant after a given period of outgassing. Combining Equations (13), (17), and (18) gives a differential equation of the form

$$\frac{dN}{dt} = \alpha - \beta N. \tag{19}$$

The substitutions $\alpha = C_0(D/\pi t)^{1/2}$ and $\beta = ne^{-\varepsilon_{\rm des}/RT}$ have been employed. This gives a solution:

$$N(t) = \alpha/\beta + N_0 e^{-\beta t}, \tag{20}$$

which gives the steady state surface concentration as:

$$N(t_{\rm og}) = \alpha/\beta = \frac{C_0(D/\pi t)^{1/2}}{ne^{-\varepsilon_{\rm des}/RT_{ss}}}. \tag{21}$$

T_{ss} is the steady-state bulk temperature of the metal and $t_{\rm og}$ is the total outgassing time. We can now calculate the normalized surface concentration as a function of outgassing time. We assume that the diffusion constant will be on the order of $10^{-7}{\rm cm}^2/{\rm s}$ and use a temperature of 150°C as in the experiment. This calculation is presented in Figure 7.

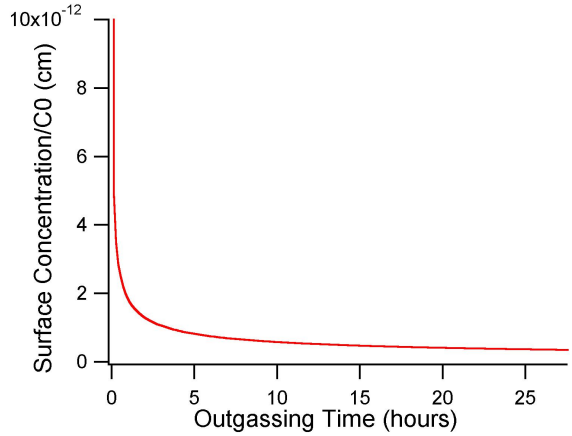

Figure 7: Surface Concentration / C_0 as a function of outgassing time for a bakeout temperature of 150°C.

Our timescale assumptions tell us that the steady-state bulk temperature doesn't change on the timescale of the laser pulse. By combining Equations (13) and (7) we get the desorbed flux as a function of temperature associated with the laser pulse and outgassing time:

$$\Gamma = C_0 \left(\frac{D}{\pi t}\right)^{1/2} \exp[-\frac{\varepsilon_{des}}{R}(T_{laser}^{-1} - T_{ss}^{-1})]. \quad (22)$$

It is our assertion that in order to initiate a discharge, the laser pulse must induce some critical flux Γ^* of desorbed material. As the thruster is allowed to outgas for a long time, the surface concentration of absorbed gas decreases, and a laser pulse must become more energetic to attain that same critical flux level. From Equation (22) we calculate that the temperature rise necessary to achieve a given Γ^*/C_0 varies in time according to:

$$T_{laser} = \{-\frac{R}{\varepsilon_{\rm des}} \log [\frac{\Gamma^*/C_0}{(\frac{D}{\pi t})^{1/2}}] + \frac{1}{T_{ss}}\}^{-1}. \quad (23)$$

The required laser pulse energy to achieve a Γ^*/C_0 chosen as 10^{-6} cm/s is plotted in Figure 8. Data from the experiment described in Section 3.1 is superimposed to show functional agreement.

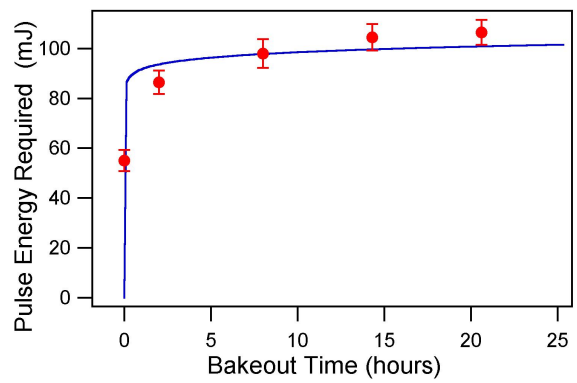

Figure 8: Required laser pulse energy to achieve a Γ^*/C_0 of 10^{-6} cm/s as a function of outgassing time for a bakeout temperature of 150°C. The experimental data from Section 3.1 is also plotted.

5 Discussion

The results of our theoretical analysis indicate that laser-induced desorption is the most likely mechanism behind the observed discharges. In terms of functional form and timescale, the results of the outgassing experiment agree fairly well with theoretical predictions. This fact further strengthens the argument that desorption is the relevant mechanism. Based on the RGA experiment, we concluded that the gas desorbed by the laser pulse is water. As a result, we have concluded that the infrared-induced breakdowns are likely caused by desorption of water into the discharge gap.

The amount of water absorbed in the backplate is not likely to be large enough to sustain significant surface concentrations for the entire lifetime of a thruster. Consequently, we do not believe that the current method of obtaining discharges is a viable technique for propulsion applications. However, it may still be possible to utilize the phenomenon of desorption to initiate GFPPT discharges. A feed system could be designed that supplies a small amount of some easily ionizable fluid to a surface in the discharge gap. This fluid could then be flash heated, either optically or with a short, high-power electrical pulse to a resistive heater, and the resulting desorption would trigger a discharge.

Thermionic emission is another alternative for controlled discharge initiation and our model suggests that it should be more practical.

Magnesium's temperature threshold for thermionic emission is higher than its boiling point as indicated in Figure 9. It is therefore not possible to extract significant thermionic currents from a magnesium surface without damaging that surface. Thermionic emission from magnesium would thus not be a viable initiation mechanism for propulsion. However, the same is not true for all materials. For example if the backplate were made out of tungsten, which has a much higher melting point than magnesium but comparable work function, it should be possible to extract significant amounts of thermionic current without damaging the surface. In addition, tungsten has a lower thermal conductivity than magnesium and thus requires less laser energy to achieve the same temperature.

In Figure 10 we plot the maximum surface temperature and thermionic electron emission in a tungsten surface versus laser pulse energy. The dashed lines indicate the melting point of tungsten. Thus, it is quite reasonable to consider a tungsten thermionic discharge initiator that would work in a fashion very similar to the current setup. This will be explored in a future experiment.

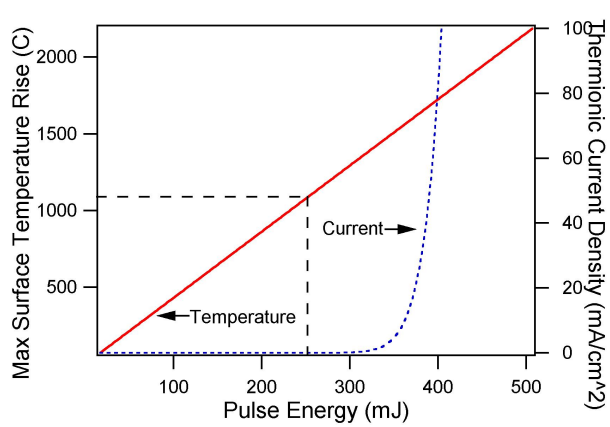

Figure 9: Maximum surface temperature and thermionic electron emission as a function of laser pulse energy for a magnesium surface. The dashed line represents the boiling point of magnesium.

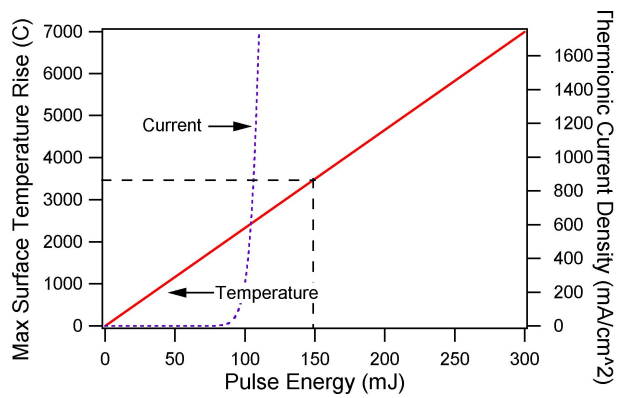

Figure 10: Maximum surface temperature and thermionic electron emission as a function of laser pulse energy for a tungsten surface. The dashed line represents the melting point of tungsten.

6 Conclusions

We have observed the phenomenon of IR-assisted breakdown in an undervoltaged PPT discharge gap and investigated three candidate mechanisms: thermionic emission, surface vaporization, and desorption.

- We have theoretically predicted that neither thermionic emission nor surface vaporization should occur at the pulse energies for which breakdowns were observed.
- We have determined through experiment and theory that desorption of water is the most likely cause of the IR-assisted PPT discharges observed thus far.
- We have also concluded that it is theoretically feasible to construct a practical discharge initiator that works on the principle of thermionic emission.

Acknowledgements

We gratefully acknowledge support from the Department of Energy's Program of Plasma Science and Technology as well as the Air Force Office of Scientific Research. We would also like to thank Prof. Szymon Suckewer and Dr. Philip Felton for their assistance.

References

[1] J.W. Berkery and E.Y. Choueiri. "Laser discharge initiation for gas-fed pulsed plasma thrusters". In 37th *Joint Propulsion Conference*, Salt Lake City, UT, 2001. AIAA-2001-3897.

[2] J. Blandino, D. Birx, J.K. Ziemer, and E.Y. Choueiri. "Performance and erosion measurements of the PT8 gas-fed pulsed plasma thruster". Technical Report EPPDyL-JPL99b,, NASA Jet Propulsion Laboratory,, August 1999.

[3] Ziemer, J.K. *Scaling Laws in Gas-fed Pulsed Plasma Thrusters*. PhD thesis, Dept. of Mechanical and Aerospace Engineering, Thesis No. 3016-T, Princeton University, Princeton, NJ, 2001.

[4] J.K. Ziemer, E.A. Cubbin, and E.Y. Choueiri. "Performance characterization of a high efficiency gas-fed pulsed plasma thruster". In 33rd *Joint Propulsion Conference*, Seattle, Washington, January 6-9, 1997. AIAA 97-2925.

[5] Yu.P. Raizer. *Gas Discharge Physics*. Springer-Verlag, 1997.

[6] S. Cohen. *Laboratory in Plasma Physics*. Princeton Plasma Physics Laboratory, 2000.

[7] S.C. Brown. *Introduction to Electrical Discharges in Gases*. John Wiley & Sons, 1966.

[8] *CRC Handbook of Chemistry and Physics, 60th Edition*. CRC Press, Inc., Boca Raton, FL, 1979.

[9] A. von Engel. *Ionized Gases*. Oxford at the Clarendon Press, 1965.

[10] J.F. Ready. *Effects of High-Power Laser Radiation*. Academic Press, 1971.

[11] J. D. Cobine. *Gaseous Conductors: Theory and Engineering Applications*. Dover Publications, 1958.

[12] Roger Nix. "An introduction to surface chemistry". www. chem.qmw.ac.uk/surfaces/scc.

[13] Ola Enquist and Anthony Stone. "Adsorption of water on MgO". *Surface Science*, **437**:239–248, 1999.

[14] Benjamin B. Dayton. Outgassing of materials. In Dorothy M. Hoffman, Bawa Singh, and III John H. Thomas, editors, "*Handbook of Vacuum Science and Technology*. Academic Press, 1998.